Calculation of the Formation Time for Microwave Magnetic Envelope Solitons

Reinhold A. Staudinger, Pavel Kabos, *Senior Member, IEEE*, Hua Xia, Byron T. Faber, and Carl E. Patton, *Fellow, IEEE*

***Abstract*—The theoretical formation and propagation properties of microwave magnetic envelope solitons were modeled from the nonlinear Schrõdinger equation without damping. Based on soliton threshold input amplitude criteria from inverse scattering theory, input amplitudes were set midpoint between the one- and two-soliton threshold values. The soliton formation time T_S was defined as the time required for the pulse amplitude to stabilize after launch. This T_S was found to be independent of the nonlinear response coefficient N and to vary as the inverse of the dispersion coefficient D. One possible way to model these T_S dependencies is through the relation $T_S \approx [T_d\ T_{\rm nl}]^{1/2}$, where T_d and $T_{\rm nl}$ are characteristic dispersion and nonlinear response times, respectively. This result suggests a simple geometric mean relation between these characteristic times.**

***Index Terms*—Delay, delay estimation, dispersive media, ferrimagnetic films, magnetostatic volume wave, magnetostatic wave, nonlinear differential equations, nonlinear magnetics, nonlinear wave propagation, solitons, yttrium iron garnet.**

I. Introduction

IN RECENT years, the observation and analysis of microwave magnetic envelope (MME) solitons formed from magnetostatic wave (MSW) signals in ferrite films have been well established (see [1] and references therein). Operationally, however, there is one critical parameter which has not been clearly defined in terms of the fundamental signal parameters, the soliton formation time, or the time measured from launch for a high power MME pulse to form a soliton. This work addresses this issue from a theoretical point of view, based on numerical calculations of pulse amplitude versus propagation time for initial square pulses obtained from the nonlinear Schrödinger (NLS) equation without damping.

Up until now, two characteristic times, a dispersion time and a nonlinear response time, have been used to establish criteria for soliton formation. The dispersion time T_d may be loosely defined as the propagation time needed for dispersion alone to produce appreciable pulse broadening. "Appreciable" is often taken to mean a doubling in the pulse width, although actual formulae for T_d usually involve assumptions about pulse shapes, spectral widths, etc. The nonlinear response time $T_{\rm nl}$ may be defined as the time for the nonlinear frequency shift to yield some specified phase change between the original low power carrier signal and the shifted carrier signal at the high power level of interest. For the analysis given below, it will prove convenient to invoke a phase change of π rad. One of the standard texts in nonlinear optics [2] invokes a phase change of 1 rad.

It is important to emphasize both these definitions involve somewhat arbitrary criteria. In addition, the time scale over which the dispersive effects become important changes with the shape of the initial pulse that is used to excite the MME signal. The dispersion time for an hyperbolic secant input pulse, for example, is a factor of 2π larger than for a square input pulse (see, e.g., [2]). Intuitively, one can argue that the initial pulse width and/or amplitude needed to produce a soliton will be such that $T_d/T_{\rm nl}$, the ratio of the dispersion time to the nonlinear response time, is on the order of unity. This is related to the requirement that the phase change caused by nonlinear response must be sufficient to compensate for the phase change caused by dispersion [3]. Suitable definitions of T_d and $T_{\rm nl}$ allow one to express this qualitative argument in terms of the $T_d/T_{\rm nl}$ ratio, which may be used to define the soliton order. In the discussion to follow, this consideration of soliton order will be made quantitative through use of the soliton eigenvalue index n from inverse scattering theory.

There are two problems with the above approach. First, the above characteristic time arguments address the conditions for solitons to be realized at some later time, not the actual time to form a soliton. Second, the observed formation times for solitons in real microwave experiments may be established empirically. These times are typically larger or smaller than either of these characteristic times, according to the particular definitions invoked.

The objective of this work was to examine the time required for an MME soliton to form. This was done from numerical calculations based on the NLS equation for signal parameters appropriate to thin magnetic films. The dependence of this formation time T_S on the two key wave packet control parameters, the dispersion coefficient, and the nonlinear response coefficient, was examined.

II. Method

The pulse propagation calculations were based on the NLS equation

$$i\left(\frac{\partial u}{\partial t}+v_g\frac{\partial u}{\partial x}\right)+\frac{D}{2}\frac{\partial^2 u}{\partial x^2}-N|u|^2u=0. \qquad (1)$$

Manuscript received June 2, 1997; revised January 9, 1998. This work was supported in part by the National Science Foundation, Grant DMR-9400276, the U.S. Army Research Office, Grant DAAHO4-95-1-0325, the National Science Foundation of China, and the Deutscher Akademischer Austauschdienst.

R. A. Staudinger, B. T. Faber, and C. E. Patton are with the Department of Physics, Colorado State University, Fort Collins, 80523 USA.

P. Kabos is with the Department of Physics, Colorado State University, Fort Collins, 80523 USA, on leave from the Slovak Technical University, Bratislava, Slovakia.

H. Xia is on leave from the National Laboratory of Solid State Microstructures, Nanjing University, Nanjing, China.

Publisher Item Identifier S 0018-9464(98)03098-2.

0018–9464/98$10.00 © 1998 IEEE

The u parameter denotes a scalar reduced dynamic magnetization amplitude $u(x,t)$ for the envelope function of the microwave wave packet which starts out as the launched square pulse at time $t = 0$. The MSW amplitude $|u|$ is related to the dynamic magnetization response $\mathbf{m}$ and is typically on the order of $|\mathbf{m}|/M_s$, where M_s is the saturation magnetization. The v_g parameter denotes the group velocity of the propagating pulse in the positive x-direction. This v_g corresponds to the slope of the MSW dispersion curve at frequency ω and wave number k at the operating point of interest. The D parameter represents the curvature of the $\omega(k)$ dispersion function. The parameter N describes the change in the MSW frequency with respect to $|u|^2$.

The results presented below are all based on numerical evaluations of pulse propagation under various conditions for values of ω, k, D, and N which match typical experimental conditions. In such work, confusion over frequency units often leads to the loss or gain of factors of 2π between various workers and between cited numerical values often given with the same units. Here, the parameters D and N will be specified explicitly in units of cm^2/rad $\times$ s and rad/s, respectively. This is related to the units of rad/s and rad/cm which apply to ω and k, respectively, even though the wave number k is usually cited simply as in units of 1/cm. There is still some inconsistency in (1) however, unless the operators $\partial/\partial t$ and $\partial/\partial x$ are assigned units of rad/s and rad/cm as well.

It is important to note that there is no damping term included in (1). The purpose here is to start with the simplest possible criteria for soliton formation and examine the formation times which follow. Without damping, the criteria for soliton formation can be obtained in analytical form from inverse scattering theory. These criteria are given below. With damping included, the problem becomes much more complicated. Of course, any complete statement on soliton formation times will require the inclusion of damping in the analysis. The present results are intended to provide guidelines for more extended work.

Microwave soliton experiments are usually done with input square pulses of some temporal width T_0 applied to an antenna in order to launch the MSW pulses in the magnetic film. Numerical simulations of pulse propagation based on the NLS equation in the form shown in (1) requires the use of initial pulses of some spatial width Γ_0 applied at some initial time. Typical experimental values for T_0 are in the 10–20 ns range [2]. In order to model experiments, the simulations were made for a spatial input width $\Gamma_0 = v_g T_0$, with T_0 set at 13 ns and the group velocity v_g set at 3.51×10^6 cm/s. These values match the experimental parameters in recent experiments by Xia *et al*. for magnetostatic backward volume wave pulses [4].

The simulations were done as follows: 1) an initial square pulse of amplitude u_0 and width Γ_0 centered at position $x = 0$ was launched at time $t = 0$. 2) An evolved pulse is then observed down line at some $t = T$. 3) This evolved pulse will correspond to some complex envelope function $u(x,T)$. 4) One determines the peak value of $|u(x,T)|^2 = |u|^2_{\max}$. 5) One then varies T, follows $|u|^2_{\max}$ as a function of T, and uses these numerical data to define a soliton formation time T_S.

From inverse scattering theory [5], the control parameter for soliton formation may be shown to be the area under the initial pulse defined by $\int u_0(x)\,dx$. The condition for the formation of a soliton which corresponds to n eigenvalues for the inverse scattering problem is

$$\int_{-\infty}^{\infty} u_0(x)\,dx > \pi(n-1/2)\sqrt{\left|\frac{D}{N}\right|}. \tag{2}$$

In the case of a square input pulse this leads to a threshold condition for the amplitude of the input pulse that is given by

$$u_{0,n}^{\text{th}} = \frac{1}{2}\frac{(2n-1)\pi}{|v_g|T_0}\sqrt{\left|\frac{D}{N}\right|}. \tag{3}$$

Equation (3) defines the threshold input amplitude for formation of a soliton from a square input pulse of width T_0 which corresponds to n eigenvalues. The $n = 1$ threshold $u_{0,1}^{\text{th}}$ corresponds to the minimum threshold amplitude for the eventual formation of a soliton. An initial amplitude at $u_{0,1}^{\text{th}}$, however, would only yield a soliton after infinite time. An initial amplitude at the next highest threshold $u_{0,2}^{\text{th}}$ would also allow the possibility of multisoliton formation because one would now enter the two eigenvalue regime of solutions. For the purposes of this analysis, an intermediate initial pulse amplitude which matches the $u_{0,n}^{\text{th}}$ value at $n = 3/2$ will be used. This condition makes intuitive sense because one is above the absolute minimum threshold at $u_{0,1}^{\text{th}}$ but still below the two eigenvalue amplitude at $u_{0,2}^{\text{th}}$.

The objective here is to determine the effect of dispersion and the nonlinear response on soliton formation time in a self consistent manner. To this end, D and N were varied in such a way that the initial amplitude u_0 was held at $u_{0,3/2}^{\text{th}}$, midway between the $n = 1$ and $n = 2$ threshold values. The condition $u_0 = u_{0,3/2}^{\text{th}}$ is operationally useful for several reasons. First, and as indicated above, this choice allows the observation of $n = 1$ solitons in a reasonable time and, at the same time, avoids the problem of $n = 2$ solitons. The second advantage has to do with the fact that the threshold for soliton formation changes with both D and N. From (3), this condition is of the form $u_0 T_0 \propto \sqrt{|D/N|}$. If one were simply to vary D or N and keep the initial $u_0 T_0$ product fixed, any observed change in the soliton formation time would be affected by the change in the threshold amplitudes defined through (3) as well as any intrinsic effects associated with the dispersion and the nonlinearity. In order to isolate the latter effects for these simulations, u_0 was adjusted to $u_{0,3/2}^{\text{th}}$ as D or N were varied with T_0 held constant.

The importance of a consistent choice for u_0 in order to obtain a soliton formation parameter T_S is demonstrated by the three graphs in Fig. 1. The plots show values of $|u|^2_{\max}$ as a function of time for three choices of u_0. For graph (a), u_0 is set at $0.5\ u_{0,3/2}^{\text{th}}$ right at the single soliton threshold. For graph (b), u_0 is set at $u_{0,3/2}^{\text{th}}$, midway between the one and two soliton threshold values. For graph (c), u_0 is set at $1.6\ u_{0,3/2}^{\text{th}}$, slightly above the two soliton threshold. The simulations were done for $D = 1.36 \times 10^3$ cm^2/rad$\times$s and $N = -6.72 \times 10^9$ rad/s, along with the $v_g = 3.51 \times 10^6$ cm/s and $T_0 = 13$ ns values stated above. These choices represent typical values for MME soliton experiments. The specific values chosen are the same as those obtained in [4]. Note that D is positive and N

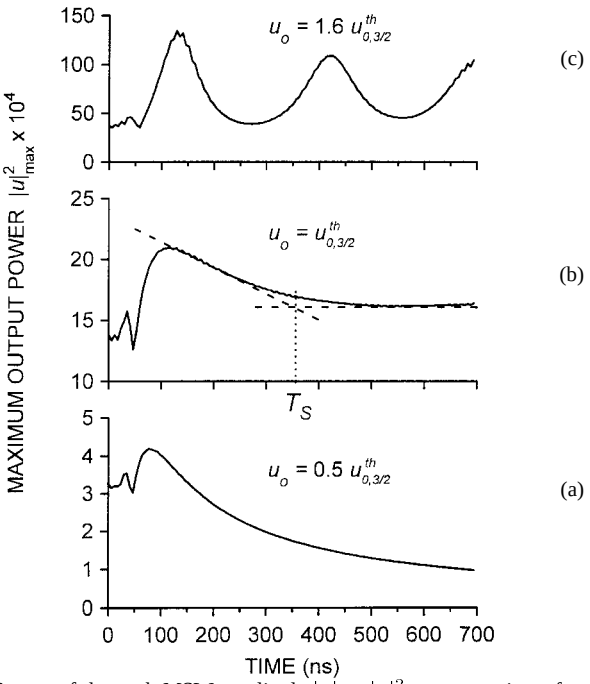

Fig. 1. Square of the peak MSW amplitude $|u|$ or $|u|^2_{\max}$ versus time after launch for three values of the initial amplitude u_0: (c) $u_0 = 1.6u^{\rm th}_{0,3/2}$, (b) $u_0 = u^{\rm th}_{0,3/2}$, and (a) $u_0 = 0.5u^{\rm th}_{0,3/2}$. The parameters for the simulation are given in the text. For scaling purposes, the $|u|^2_{\max}$ values are multiplied by 10^4, as indicated.

is negative. For magnetostatic backward volume waves, the dispersion has positive curvature and the frequency shift with increasing amplitude is negative.

Except for the common formation response during the first 50 ns or so, the three traces demonstrate different behaviors for the evolving pulses. Graph (a) shows a steady decay which never levels off to some steady state amplitude value. Here, even though u_0 is right at the single soliton threshold, the *time* for the soliton to form is infinite. The situation is different for graph (b) and u_0 at $u^{\rm th}_{0,3/2}$. Here, the simulations show a more or less well-defined time at which $|u|^2_{\max}$ assumes a relatively constant amplitude. For times greater than about 350 ns, the amplitude in graph (b) has leveled off and one may consider the soliton to be completely formed. Graph (c) shows the effect of a larger value u_0 on the $|u|^2_{\max}$ versus time response. Here, one obtains a breathing effect typical of solitons well above threshold.

Graph (b) of Fig. 1 provides the basic definition of the soliton formation time T_S which will be used for the results to follow. The intersection of the two dashed lines for the 150–250 ns decay regime and the steady state regime above 500 ns define this T_S. This is indicated by the vertical dotted line. Of course, the time scales will vary somewhat as the parameters D and N are varied. The main objective here is to have a consistent convention for the determination of a soliton formation time. Since the formation of a soliton is not an abrupt effect, it is clear that there can be no precise value T_S. The present definition will serve the purpose to study the effect of D and N on this time.

The dependence of the formation time T_S on the dispersion parameter D and the nonlinear response parameter N was obtained from two different sets of simulations. In the first set of simulations, N was changed in a range from -3.5×10^9 rad/s to -7.5×10^9 rad/s and D was held at a constant value of 1.36×10^3 cm^2/rad $\times$ s. The values for group velocity and initial pulse width were also held constant at $v_g = 3.51 \times 10^6$ cm/s and $T_0 = 13$ ns. These values are typically used in experiments. For each run, the chosen N-value was used to calculate $u^{\rm th}_{0,3/2}$ and this value was used as the input amplitude u_0 for the pulse. Simulations were then run to obtain curves of the sort shown in Fig. 1(b) and the T_S-value was determined accordingly. The result of this first set of simulations consisted of numerical results for T_S as a function of N at fixed D. The second set of simulations followed the same procedure, except that now D was changed while N was held constant. The dispersion parameter was varied in the range 0.5×10^3 cm^2/rad$\times$s $< D < 2.5 \times 10^3$ cm^2/rad $\times$ s and N was held at a constant value of $N = -6.72 \times 10^9$ rad/s. This range of values is typical for MME soliton experiments. The result of this second set of simulations then consisted of numerical results for T_S as a function of D at fixed N.

The results of these simulations and further discussion based on these results will be given in the next section. Before these numerical results are considered, however, it is useful to review the expected connections between the soliton formation time and the D and N parameters. The vehicle for these connections will be the dispersion time parameter T_d and the nonlinear response time parameter $T_{\rm nl}$ introduced at the beginning of this paper. The definitions for these characteristic times for square input pulses translate into the following [1]:

$$T_d = \frac{v_g^2 T_0^2}{2\pi |D|} \tag{4}$$

$$T_{\rm nl} = \frac{\pi}{|N||u_0|^2}. \tag{5}$$

The important connection between T_d, $T_{\rm nl}$, and the soliton formation time comes from the $|u_0|^2$ denominator term in (5), the threshold condition from (3), and the use of a specific value of u_0 equal to $u^{\rm th}_{0,3/2}$. Note that under these conditions, one immediately obtains an additional condition $T_{\rm nl} = 2T_d$.

Now consider the effect of changing N in the above scenario. According to (3), an increase in N results in a decrease in $u^{\rm th}_{0,3/2}$ and hence in the u_0 used for the simulations. All the other factors in (3), including D, are held constant. This means that the product $|N||u_0|^2$ will remain constant and, from (5), $T_{\rm nl}$ will also remain constant. From the condition $T_{\rm nl} = 2T_d$, T_d will remain constant as well. With both characteristic times unchanging, therefore, one expects the simulation to produce a soliton formation time T_S which is also unchanging.

For the second scenario where D is changed and N is held constant, one obtains a different result for the characteristic times. Here, from (3), $(u^{\rm th}_{0,3/2})^2$ scales with D. This means, from (4) and (5), and with u_0 equal to $u^{\rm th}_{0,3/2}$, that both T_d and $T_{\rm nl}$ will scale with $1/D$ and decrease proportionately as D is increased. From these dependencies, one expects the soliton formation time T_S to be an inverse function of D as well.

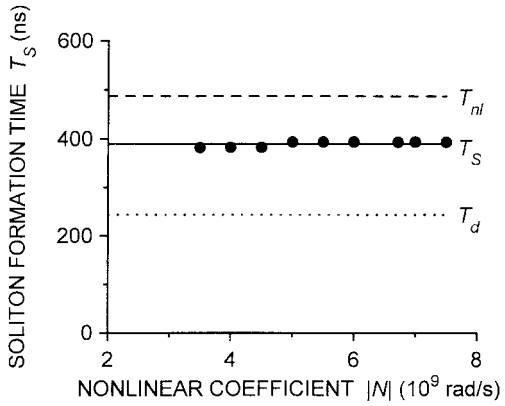

Fig. 2. Soliton formation time T_S as a function of the absolute value of the nonlinear response coefficient N, shown as $|N|$ for the first series of simulations discussed in the text. The solid circles show the calculated T_S-values. The solid line shows the best horizontal line fit to the numerical T_S data. The dotted and dashed lines show the corresponding dispersion time T_d and the nonlinear response time $T_{\rm nl}$ as a function of $|N|$.

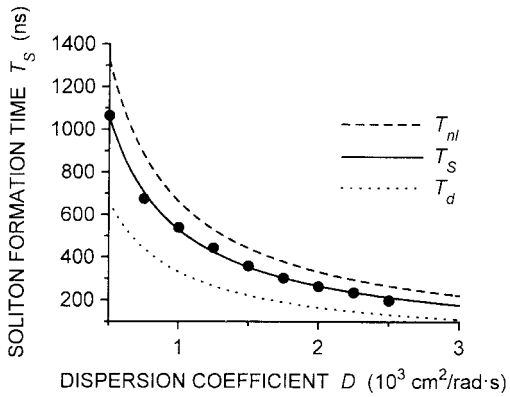

Fig. 3. Soliton formation time T_S as a function of the dispersion parameter D for the second series of simulations discussed in the text. The solid circles show the T_S-values. The solid line shows a best C/D fit to the numerical T_S data. The constant C can be calculated to be 5.3×10^{-4} cm^2/rad. The dotted and dashed lines show the corresponding dispersion time T_d and the nonlinear response time $T_{\rm nl}$ as a function of D.

III. Numerical Results

Fig. 2 shows the results from the first set of simulations described above. The soliton formation time T_S was obtained from numerical data of the sort shown in Fig. 1 for a range of values for the nonlinear response coefficient N. The solid circles show the T_S results. The dotted and dashed lines show the corresponding variations in the dispersion time T_d and the nonlinear response time $T_{\rm nl}$ from (4) and (5). The solid line through the T_S-values represents a best fit horizontal line through these numerical data points. The horizontal axis of Fig. 2 is in terms of $|N|$. Recall that the N-parameter is negative for the backward volume wave configuration chosen for these simulations.

The soliton formation time T_S and the two characteristic times $T_{\rm nl}$ and T_d shown in Fig. 2 are all constant and independent of N, subject to the procedure used for the simulation as described above. This result is expected, of course, from the choice of an initial amplitude based on (3) and the condition $u_0 = u_{0,3/2}^{\rm th}$. The unexpected result is in the position of T_S relative to $T_{\rm nl}$ and T_d. The simulation results give a T_S-value of about 390 ns. This value is between T_d and $T_{\rm nl}$ and somewhat above the mean value of these two characteristic times. Note that the T_d and $T_{\rm nl}$ values in Fig. 2 are 244 and 488 ns, respectively.

Fig. 3 shows the results from the second set of simulations. The soliton formation time T_S was obtained from numerical data of the sort in Fig. 1, but now for a range of values for the dispersion parameter D. The format is the same as for Fig. 2. The solid circles show the T_S results. The dotted and dashed lines show the corresponding variations in the dispersion time T_d and the nonlinear response time $T_{\rm nl}$ from (4) and (5). The solid line through the T_S values represents a best fit through the numerical data points for a functional dependence of the form $T_S = C/D$, with C equal to 5.3×10^{-4} cm^2/rad.

The variations in T_S and the two characteristic times T_d and $T_{\rm nl}$ with D in Fig. 3 are rather different from the constant values shown as a function of $|N|$ in Fig. 2. The good fit of the $T_S = C/D$ equation to the T_S-values demonstrates that the soliton formation times obtained from numerical simulation have the same basic functional dependence on D as do T_d and $T_{\rm nl}$. Recall that for the second simulation scenario, both T_d and $T_{\rm nl}$ vary as $1/D$. It is also important to note that the actual numerical values of T_S from the simulations fall between T_d and $T_{\rm nl}$ and are somewhat above the arithmetic mean value of these two characteristic times.

IV. Analysis and Discussion

Recall that the original objective of the present analysis was to perform a consistent numerical analysis to obtain the soliton formation time as a function of D and N. The numerical results are given above. The purpose of this final section is to examine possible general dependencies suggested by these numerical data.

As a starting point, note that two simple conclusions can be drawn from the results of the last section. First, it was found for the second scenario in which D was varied, that T_S changes with D according to

$$T_S = \frac{C}{D}, \qquad C = 5.3 \times 10^{-4} \text{ cm}^2/\text{rad}. \tag{6}$$

Equation (6) also matches the results from the first scenario simulations and the numerical results in Fig. 2. Second, the results from both scenarios indicate that the soliton formation time T_S is always between the two characteristic times T_d and $T_{\rm nl}$ as defined and discussed above. This, in itself, is a noteworthy and potentially useful result. This result goes beyond previous arguments based on the condition $T_d = T_{\rm nl}$ for soliton formation. From the discussion in Section II, the $T_d = T_{\rm nl}$ condition is equivalent to an input amplitude constraint $u_0 = u_{0,1}^{\rm th}$. Under this constraint, however, the soliton formation time is infinite. This connection was shown explicitly in Fig. 1(a) through an amplitude which continues to decay with time and never levels off.

The key result from the simulations presented above is the $1/D$ dependence of the soliton formation time as expressed

in (6). It would be useful, however, to consider further the connection between this result and the functional dependence of T_S on the characteristic times T_d and $T_{\rm nl}$. In order to obtain such a connection, one must consider the explicit D-dependencies of T_d and $T_{\rm nl}$, subject to the $u_0 = u^{\rm th}_{0,3/2}$ constraint on which the simulations were based. The dispersion time T_d is given by (4). From the discussion of Section II, the $u_0 = u^{\rm th}_{0,3/2}$ constraint yields a $T_{\rm nl}$ which is simply equal to $2T_d$. Both characteristic times, therefore, vary as $1/D$. Perhaps the simplest way to combine T_d and $T_{\rm nl}$ to produce a $T_S(T_d, T_{\rm nl})$ function with an overall $1/D$ dependence is to write T_S in terms of the geometric mean of these characteristic times and according to

$$T_S = K\sqrt{T_d T_{\rm nl}} = K\sqrt{2}T_d = K\left[\frac{v_g^2 T_0^2}{\pi\sqrt{2}}\right]\frac{1}{D} = \frac{C'}{D}. \quad (7)$$

The numerical value of the square bracket term in (7) is 4.69 $\times$ 10^{-4} cm^2/rad. If one assumes that the geometric mean formulation is correct and that (7) provides a physical basis for the numerical results summarized in (6), one may set C' equal to C and obtain K as 1.13.

It is possible, of course, to construct other functions of T_d and $T_{\rm nl}$ which are consistent with (6). The function $T_S = K(T_d T_{\rm nl}^2)^{1/3}$, for example, also matches the empirical result of (6) and yields a K-value of 1.01. Functions of the form $T_S = (aT_d + bT_{\rm nl})$ would also work. The main point is that numerical simulations of the sort presented here, performed under various systematic constraints on the initial pulse amplitude, may be used to explore possible connections between the soliton formation time and the characteristic times for the soliton system.

V. Summary and Conclusion

The present results show that the time required to form a stable soliton from an initial rectangular input pulse in a nonlinear medium with no damping can be modeled by a simple geometric mean relation of the two characteristic times T_d and $T_{\rm nl}$ as defined in (4) and (5). Previous work has only given the condition $T_{\rm nl} \approx T_d$ as a necessary condition for soliton formation, but this result says nothing about the actual time for a soliton to form. The present analysis provides a specific working equation for the actual time for the soliton to form. This condition works for two very different numerical modeling scenarios. Other $T_S(T_d, T_{\rm nl})$ functions are also possible, of course. The determination of a unique $T_S(T_d, T_{\rm nl})$ connection, if such a connection exists, will require further numerical analysis with and without special constraints on the input amplitude.

It is important to note that the decay in the pulse amplitude due to various loss mechanisms in the material has been completely neglected. It is clear that damping would have an additional effect on the response curves of the sort shown in Fig. 1 and that a new definition of soliton formation time would be needed. Further work on soliton formation time in the presence of damping is presently underway.

Acknowledgment

The authors gratefully acknowledge Prof. B. A. Kalinikos and Prof. A. N. Slavin for helpful discussions. Both reviewers are acknowledged for pointing out the possibility of applicable $T_S(T_d, T_{\rm nl})$ functions other than the geometric mean function.

References

[1] N. G. Kovshikov, B. A. Kalinikos, C. E. Patton, E. S. Wright, and J. M. Nash, "Formation, propagation, reflection, and collision of microwave magnetic envelope solitons in yttrium iron garnet films," *Phys. Rev. B*, vol. 54, pp. 15210–15223, 1996.

[2] G. P. Agrawal, *Nonlinear Fiber Optics*. San Diego, CA: Academic, 1995, pp. 60–63.

[3] M. Chen, M. A. Tsankov, J. M. Nash, and C. E. Patton, "Backward-volume-wave microwave-envelope solitons in yttrium-iron-garnet films," *Phys. Rev. B*, vol. B49, pp. 12773–12790, 1994.

[4] H. Xia, P. Kabos, C. E. Patton, and H. E. Ensle, "Decay properties of microwave magnetic envelope solitons in yttrium iron garnet films," *Phys. Rev. B*, vol. B55, pp. 15 018–15 025, 1997.

[5] A. Hasegawa and Y. Kodama, "Signal transmission by optical solitons in monomode fibers," *Proc. IEEE*, vol. 69, no. 9, pp. 1145–1150, 1981.